Cryst. Res. Technol.	**33**	1998	2	183–195

N. Lovergine[1], P. Prete[2], G. Leo[2], L. Calcagnile[1], R. Cingolani[1], A. M. Mancini[1], F. Romanato[3], A. V. Drigo[3]

[1] Istituto Nazionale per la Fisica della Materia (INFM), Unità di Lecce and Dipartimento di Scienza dei Materiali, Università di Lecce, Via per Arnesano, I-73100 Lecce, Italy
[2] IME-CNR, Via per Arnesano, I-73100 Lecce, Italy
[3] INFM, Unità di Padova and Dipartimento di Fisica "G. Galilei", Universita di Padova, Via Marzolo 8, I-35131 Padova, Italy

MOVPE Growth of Wide Band-Gap II–VI Compounds for Near-UV and Deep-Blue Light Emitting Devices

We report on the growth by metalorganic vapour phase epitaxy of high structural and optical quality ZnS, ZnSe and ZnS/ZnSe multiple quantum well (MQW) based heterostructures for applications to laser diodes operating in the 400 nm spectral region. High purity ^{t}BuSH, ^{t}Bu$_2$Se and the adduct $Me_2Zn : Et_3N$ were used as precursors of S, Se and Zn, respectively. The effect of the different MOVPE growth parameters on the growth rates and structural properties of the epilayers is reported, showing that the crystallinity of both ZnS and ZnSe is limited by the kinetics of the incorporation of Zn, S and Se species at the growing surface. Very good structural and optical quality ZnS and ZnSe epilayers are obtained under optimized growth conditions, for which also dominant (excitonic) band-edge emissions are reported. The excellent ZnS and ZnSe obtained by our MOVPE growth matches the stringent requirements needed to achieve high quality ZnS/ZnSe MQWs. Their structural properties under optimized MOVPE conditions are shown to be limited mostly by the formation of microtwins, a result of the intrinsic high lattice mismatch involved into the ZnS/ZnSe heterostructure. Despite the large amount of defects found, the optical quality of the MQWs turned out to be high, which made possible the full characterization of their electronic and lasing properties. In particular, photopumped lasing emission up to 50 K in the 3.0 eV energy region are reported for the present MQWs heterostructures under power excitation density above 100 kW/cm^2.

Introduction

The ever increasing technological needs for opto-electronic devices, such as light emitting diodes (LEDs) and laser diodes (LDs), operating in the near-UV and deep-blue spectral regions of light continues to foster much of the current research activities on the epitaxy of wide band-gap semiconductor heterostructures. Indeed, since the demonstration by Hua et al. at 3M of the very first II–VI compounds based LD, which used a ZnSe/ZnCdSe multiple quantum well (MQW) active region to achieve stimulated emission in the blue-green wavelength range (460–510 nm) of the visible light, there has been a steady interest in the search for new II–VI based heterostructures capable of laser emission at even shorter wavelength: i.e., in the deep-blue and UV spectral region ($\lambda < 420$ nm). After the successful demonstration by Nakamura in 1995 of the first III-nitrides based LD operating at around 405 nm, the race for lasers with shorter emission wavelengths and longer lifetimes is still open between II–VI and III-nitrides wide band-gap semiconductor compounds.

Amongst II–VI based heterostructures with potential applications to the realization of highly efficient deep-blue emitting LDs, many efforts have been recently focusing on S-containing II–VI heterostructures, such as ZnS/ZnSe MQWs and short-period superlattices (SLs); these structures were shown by TAGUCHI et al. to have band-edge emissions at wavelength much shorter than 460 nm. However, very little has been reported so far on the electronic properties and lasing emissions of these heterostructures, primarily because of the difficulties encountered by both molecular beam epitaxy and metalorganic vapour phase epitaxy (MOVPE) methods in the preparation of high optical and structural quality ZnS/ZnSe SLs.

In what concerns MOVPE, the occurrence of unwanted pre-reactions between the common II-group species and many S- and Se-precursors along with the lack of the neccessary purity of both alkyls and gaseous sources used in the process have long been some of the factors limiting the overall structural and electronic quality of the MOVPE-grown ZnS/ZnSe based heterostructures. Also, the combination of precursors used in the process and their different thermal stability strongly affects both the growth temperatures and the effective elemental VI/II stoichiometry ratios achieved in the vapour phase, which in turn determine both the microscopic properties of the epilayers (i.e., the type and density of defects as well as the overall impurity content) and the sharpness of the ZnS/ZnSe interfaces. The initial MOVPE method for growing ZnS and ZnSe epilayers required the combination of H_2S and H_2Se with a zinc alkyl such as dimethyl-zinc (Me_2Zn) or diethyl-zinc (Et_2Zn), allowing growth temperatures as low as 290 °C. However, the use of the VI-group hydrides is far from ideal, due to their high toxicity and the limited extent to which these gaseous sources can be purified. Moreover, the use of the hydrides in combination with the II-group alkyls invariably lead to extensive pre-reactions, which adversely affected both crystalline and optical qualities of the epilayers. Dialkyl-sulfides and -selenides, such as diethyl-sulfide and dimethyl-selenide, are being used by several groups as alternative S and Se sources, as these precursors are less toxic than the corresponding hydrides and, additionally, they do not suffer from pre-reactions with the II-group alkyls. However, growth temperatures in excess of 450 °C are required in this case, which are detrimental for both the interface abruptness and the optical quality of the heterostructures. The use of VI-group precursors containing higher and more stable hydrocarbon radicals, such as t-buthyl ar allyl groups, was suggested in recent years as a strategy for reducing the pyrolysis temperatures of the precursors by the weakening of the M^{VI}-C bonds (where, M^{VI} = S, Se). In this respect, ditertiary-buthyl-selenide ($^tBu_2Se$) has become the preferred Se precursor, as it was shown by KUHN et al. that it allows ZnSe growth temperatures below 350 °C. Similarly, the use of tertiary-buthyl-thiol (^{t}BuSH) as a suitable low growth temperature precursor was first reported by NISHIMURA et al. for the MOVPE growth of $Cd_xZn_{1-x}S$, but pre-reactions between ^{t}BuSH and the II-group alkyls were observed by the authors. In agreement to what initially reported by WRIGHT et al., LOVERGINE et al. and LEO et al. further reported that the combination of ^{t}BuSH with the adduct dimethyl-zinc:triethyl-ammine ($Me_2Zn : Et_3N$) strongly reduces pre-reactions between these species, also allowing the low temperature (below 340 °C) growth of high optical quality ZnS epilayers. The use of $Me_2Zn : Et_3N$ as a Zn source has also become a standard in the growth of ZnSe as it suppresses the otherwise residual pre-reactions between $^tBu_2Se$ and Me_2Zn (HAHN et al.). Moreover, the $Me_2Zn : Et_3N$ adduct can be obtained of higher purities with respect to Me_2Zn alkyl batches, thus matching the high purity levels expected in the halide-free Se sources (i.e., $^tBu_2Se$), which nowadays begin to be available.

In the present work, we report on the growth by low-pressure MOVPE of ZnS, ZnSe and ZnS/ZnSe MQWs heterostructures using the above mentioned S, Se and Zn alkyl precursors. The combination of precursors chosen and their purity allows us to match the stringent requirements needed for the MOVPE growth of high structural and optical quality epilayers and MQWs. Results on the structural and optical characterization of ZnS, ZnSe and ZnS/ZnSe MQWs samples will be thus presented, along with the effects of the different growth parameters on the heterostructure properties. This study has also allowed us to optimize the growth of fairly high quality ZnS/ZnSe MQWs, whose electronic and lasing properties have been thus fully characterized. The main issues limiting the applications of these heterostructures to the realization of blue emitting LDs will be finally pointed out.

Experimental

ZnS/ZnSe based heterostructures were grown by low pressure MOVPE in an Aixtron model AIX 200RD horizontal reactor. High purity ^{t}BuSH, ^{t}Bu$_2$Se and the adduct Me$_2$Zn : Et$_3$N, as supplied from Epichem, Ltd. (UK), were used as metalorganic precursors of S, Se and Zn, respectively. The ^{t}Bu$_2$Se and ^{t}BuSH batches used thoughout the present work were of the halide-free type, as their synthesis avoided the use of Grignard's reagents.

ZnS, ZnSe and ZnS/ZnSe-based MQW heterostructures were deposited grown on LEC-grown (100)GaAs substrates of semi-insulating (resistivity $>10^7\ \Omega \cdot$ cm) type. Immediately before loading into the reactor chamber the substrates were first degreased in isopropanol vapour and than wet-etched for 8 min at around 40 °C in a $H_2SO_4 : H_2O_2 : H_2O$ (4 : 1 : 2) solution, after which they were thoroughly rinsed in 18.2 MΩ de-ionized water and finally dried under pure N_2. In order to chemically reduce the oxides left on the GaAs surface by the etching solution, an in-situ thermal treatment under hydrogen flow was routinely performed on the substrates, after loading into the reactor chamber. Optimal temperatures between 510 °C and 550 °C were chosen for the GaAs in-situ heat treatment, according to what previously reported by Gebhardt et al. and Leo et al. (1996).

Both single epitaxial layers and MQW heterostructures were grown under low pressure ($P_C = 304$ mbar) conditions, whereas a total H_2 flow rate of 7.4 sl/min was used for all growth runs, achieving an average gas velocity through the reactor chamber of ∼16 cm/sec. These conditions were shown to be sufficient to achieve sharp interfaces when growing ZnS/ZnSe MQWs.

ZnS and ZnSe layers were grown under S- and Se-rich vapour phase conditions, respectively; the actual molar flow rates used for each alkyl were calculated according to saturated vapour pressure data previously reported by Lovergine et al. for ^{t}BuSH and Irvine et al. for ^{t}Bu$_2$Se and Me$_2$Zn : Et$_3$N. Precursor molar flow rates were thus kept fixed at around 103 μmol/min for ^{t}BuSH and 287 μmol/min for ^{t}Bu$_2$Se, whereas, the Zn source transport rate was varied between about 3.6 and 25 μmol/min. These values allowed to growth with VI/II precursor molar flow ratios ($R_{VI/II}$) between approximately 4 and 30 for ZnS and within the 12−80 range for ZnSe. Finally, the epilayer growth temperatures were varied in the 290 °C−370 °C interval.

The crystallinity of ZnS and ZnSe epilayers grown on GaAs was assessed as a function of growth conditions by means of either double-crystal x-ray diffraction (DC-XRD) or Rutherford backscattering spectrometry (RBS) in ion-channeling conditions. Finally, the

defect type and distribution occurring in ZnS/ZnSe MQW heterostructures were analyzed by conventional transmission electron microscopy (TEM) by using a JEOL 2000 FX microscope. To this purpose bright-field and dark-field observations were done at 200 keV on ⟨110⟩ oriented cross-sections prepared by mechano-chemical thinning, followed by low-temperature Ar ion-milling in a Gatan 600 Duo-mill system.

High resolution continuous wave photoluminescence (PL) measurements were performed between 10 K and room temperature on both ZnS, ZnSe and ZnS/ZnSe MQWs samples. To this purpose, the samples were excitated by the UV line (1 W at 275.4 nm) of a large frame Ar^+ laser. PL emissions were recorded from the samples in a backscattering configuration, dispersed by a 0.85 m double monochromator, and finally detected by a cooled GaAs photon counting. The overall spectral resolution achieved was always better than 0.5 meV. High excitation PL measurements were carried out on ZnS/ZnSe MQWs as a function of excitation power density in order to study the threshold for lasing. Photopumping was achieved by using the third harmonic (355 nm) of a Nd : YAG laser, delivering laser pulses of 5 n sec at a repetition rate of 10 Hz. Samples in the form of cleaved cavities having average widths of ∼1 mm were realized and measured in both the backward and edge configurations. The injection rate on the sample surface was varied by using a set of calibrated neutral filters. The radiation emitted by the sample was dispersed by means of a 0.45 m double monochromator and finally detected by a photomultiplier tube.

Results

Fig. 1 shows the dependence of the ZnSe and ZnS growth rates on MOVPE temperature in an Arrhenius plot. It appears that ZnSe and ZnS growth processes are both thermally

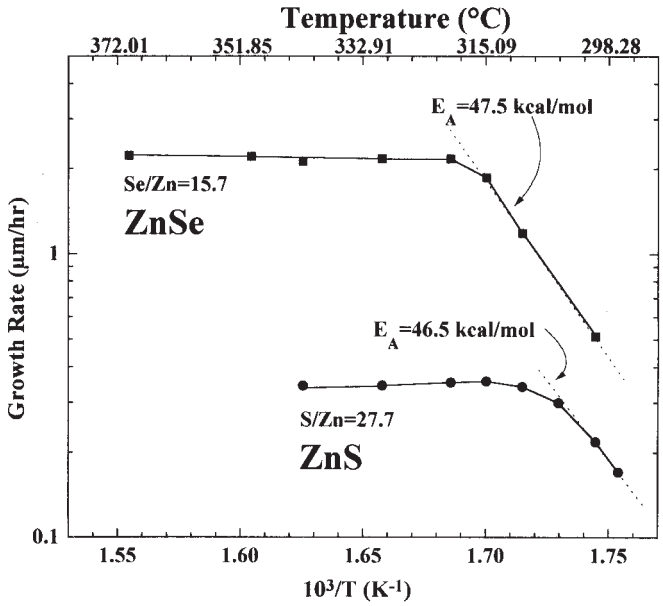

Fig. 1. Arrhenius plot of the ZnSe and ZnS growth rates as a function of temperature. The S/Zn and the Se/Zn molar flow ratios are indicated for each curve. The low temperature activation energy results to be 46.5 ± 0.5 kcal/mol for ZnS and 47.5 ± 0.5 kcal/mol for ZnSe

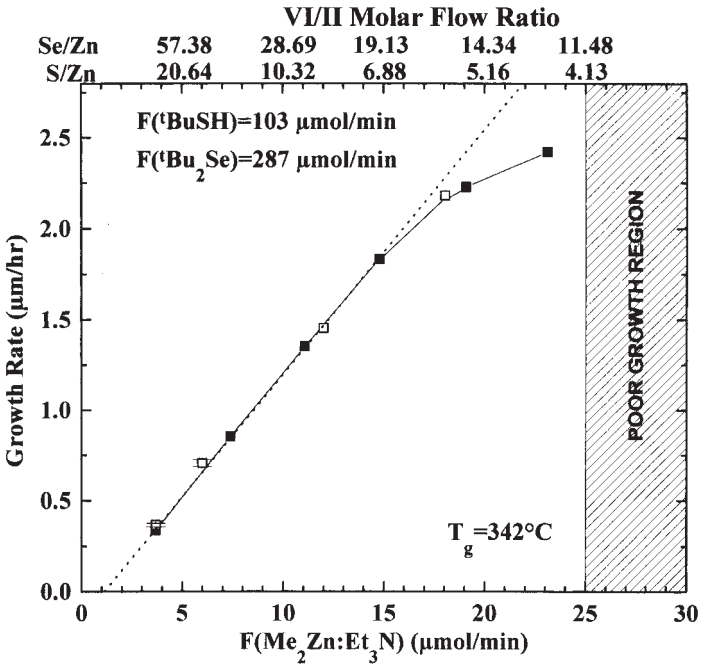

Fig. 2. Epilayer growth rates for ZnS (full points) and ZnSe (empty points) as a function of the Zn adduct molar flow rate. The corresponding S and Se alkyl trasport rates are indicated in the figure. The growth temperature is 342 °C for all data

activated at relatively low temperature (below 315 °C), where they show an apparent activation energy of about 47 kcal/mol. On the contrary, at higher temperatures the growth rates remain constant, indicating that the growth is mass transport limited. Indeed, Fig. 2 shows that, at 342 °C and for Zn adduct transport rates below ∼15 µmol/min, the growth rates of ZnSe and ZnS both depend linearly on the $Me_2Zn:Et_3N$ molar flow; moreover, the growth rate data lay on the same straight line, despite the different S- and Se-alkyl trasport rates used for the two materials. These results show that, above about 315 °C, the mass transport of the Zn alkyl is the actual growth limiting mechanisms under S- and Se-rich vapour phase conditions. Moreover, the $Me_2Zn:Et_3N$ molecule is known to be fully dissociated in the vapour phase, even at relatively low temperatures (Kahn et al.). Thus, the 47 kcal/mol activation energy shown in the Arrhenius plot of Fig. 1 should be ascribed to a kinetic step involving the Me_2Zn alone, the S and Se precursors being much less stable than the Zn alkyl, such that their interchange would have no effects on the epilayer growth rates even at temperatures as low as 290 °C.

Fig. 2 shows that the epilayer growth rates deviate from linearity if the amount of Zn adduct transported into the vapour phase is greater than 15 µmol/min, such that by further increasing the $Me_2Zn:Et_3N$ molar flow a saturation of the growth rates is observed for ZnS. Noteworthy, for Zn alkyl molar flow rates above ∼25 µmol/min, ZnS layers of very poor crystalline quality and dull surface appearence are obtained. It appears that, despite the use of the Zn adduct and low pressure into the reactor chamber, residual pre-reactions between $Me_2Zn:Et_3N$ and ^{t}BuSH possibly occur, under the above

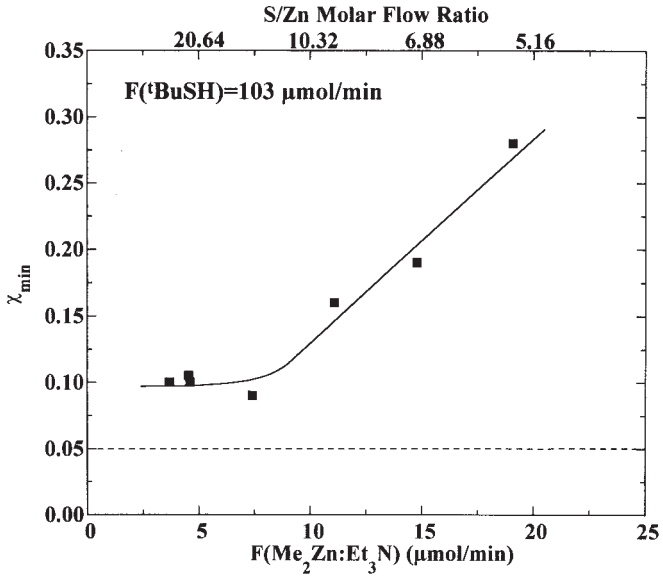

Fig. 3. The RBS surface minimum yield χ_{min} of ZnS epilayers grown at 342 °C is reported as a function of the Zn adduct molar flow rate. The horizontal dotted line at $\chi_{min} = 0.05$ represent the value expected for a perfect ZnS crystal

conditions. On the contrary, no hints of pre-reactions were apparently observed for the ZnSe growth, even under the highest Zn adduct molar flow rates used in the present study, in agreement with what usually reported by other authors in the literature. More details on this matter will be reported elsewhere.

The crystalline quality of the epilayers has been systematically investigated (Leo et al., 1996) by looking at the so-called RBS surface minimum yield (χ_{min}), that is the channeling back-scattering yield just behind the surface peak of the epilayer RBS spectra, normalized to the corresponding random yield. Fig. 3 shows the dependence of χ_{min} as a function of the $Me_2Zn:Et_3N$ molar flow for ZnS epilayers grown at 342 °C. The crystalline quality is best for Zn alkyl transport rates below 8 µmol/min, for which $\chi_{min} = 0.10$, but it worsen at higher $Me_2Zn:Et_3N$ molar flow. As the epilayer growth rate encreases almost linearly with the Zn transport, the Zn and S atoms will have correspondingly less time to find their lattice sites on the growing surface, at the relatively low growth temperatures used in the present work; the observed deterioration of the crystal perfection can be thus explained. As a matter of fact, RBS measurements performed on epilayers grown at different temperatures show improved crystalline quality with increasing MOVPE temperature. Still the best surface crystalline quality we achieved for ZnS epilayers corresponds to $\chi_{min} = 0.10$, i.e. higher than the 0.05 value expected for a perfect (defect-free) ZnS crystal. In fact, TEM observations (see below) confirm that even for ZnS/GaAs heterostructures grown under optimized conditions, extended defects still occur as a result of the plastic relaxation of the +4.6% lattice misfit between ZnS and GaAs (Leo et al, 1997).

In Fig. 4 we report the behaviour of the full width at half maximum (FWHM) value of the DC-XRD (400) peak for 1 µm thick ZnSe epilayers grown at $R_{VI/II} = 15.7$ as a

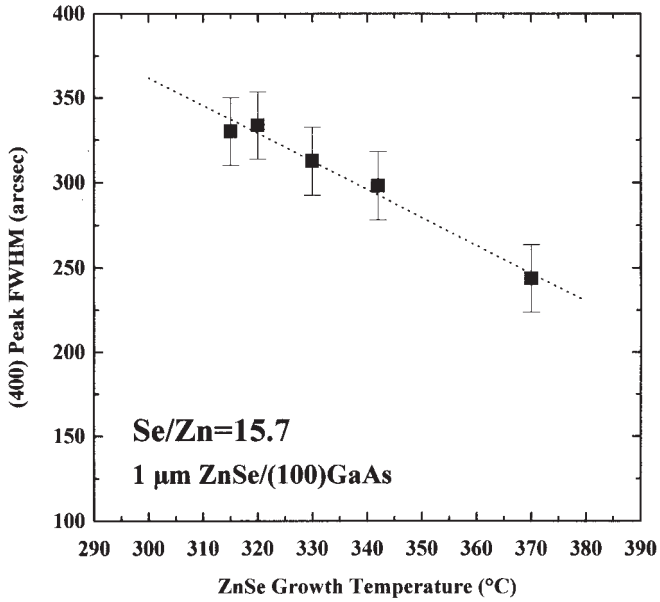

Fig. 4. Values of the full width at half maximum (FWHM) measured for the DC-XRD (400) peak of a 1 μm thick ZnSe epilayer as a function of the growth temperature

function of their growth temperature. It appears that the structural perfection of ZnSe, whose growth rate is constant between 310 °C and 370 °C (see Fig. 1), improves almost linearly by encreasing the MOVPE growth temperature, such that relatively good quality epilayers having FWHM $\approx$ 240 arc sec can be grown at 370 °C. Still this value is much higher than the FWHM value expected for a perfect (defect-free) ZnSe epilayer of the same thickness, which is in turn well above the critical value for the ZnSe lattice strain relaxation (Gebhardt et al.): the presence of dislocations is thus expected in the layers, accounting for most of the observed DC-XRD peak broadening. More details on the above DC-XRD and RBS measurements were reported by Giannini et al. and Leo et al. (1997).

Fig. 5a shows a typical 10 K PL spectrum of a 0.71 μm thick ZnSe epilayer grown at 315 °C and $R_{\mathrm{VI/II}} = 47.1$. The PL emission appears to be dominated by a strong peak at 2.802 eV (X_{1s}) in the near band-edge region of ZnSe. A comparison with 10 K absorption measurements performed on the same sample shows that this peak can be ascribed to a free exciton recombination. Furthermore, the weak peak (X_{2s}) at 2.816 eV in the PL spectrum can be identified as the 2 s state exciton line. A neutral donor bound exciton line (I_2) ascribed to Cl can be seen at around 2.976 eV, its intensity being lower than the X_{1s} line, suggesting that the amount of unintentional Cl incorporated into the epilayer is low. Indeed, only a weak donor acceptor pair recombination band (DA) can be detected in the spectrum at 2.716 eV, followed by its phonon replica (DA-1LO) at 2.685 eV, whereas a contribution ascribable to a free-to-bound acceptor transition (e, A^0) appears at 2.740 eV. Finally, two emission lines at 2.775 eV and 2.603 eV can be resolved in Fig. 5a and identified with the extended defects (i.e., dislocations) related I_{v}^0 and Y_0 transitions, respectively (Shahzad et al.); also, a phonon replica of the latter

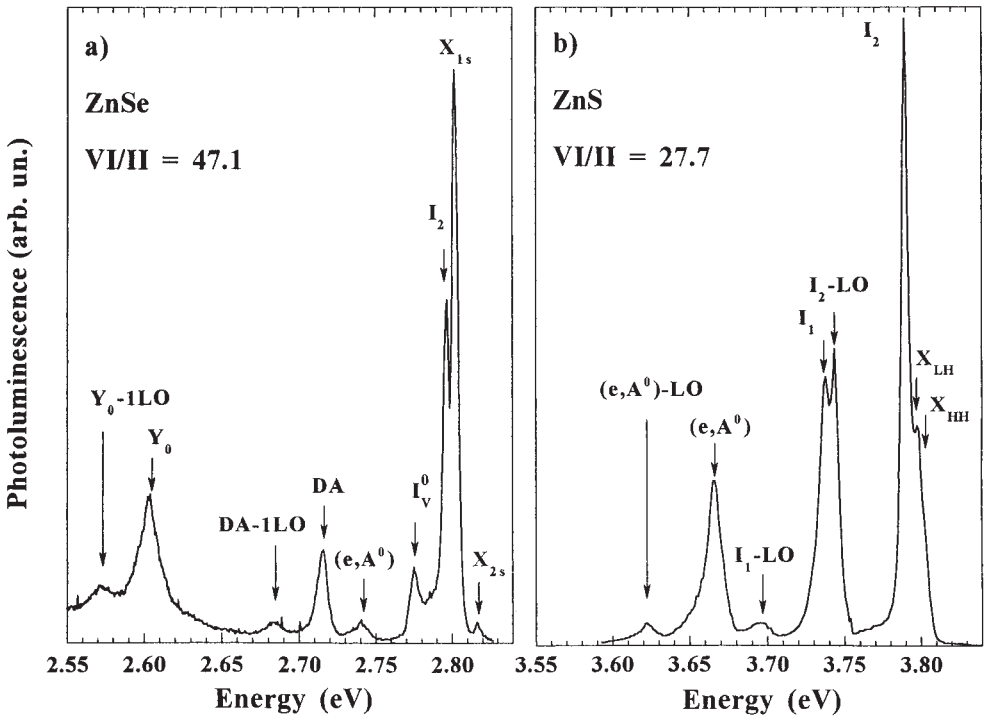

Fig. 5. Typical 10 K near band-egde PL spectra of (a) a 0.71 μm thick ZnSe epilayer grown at 315 °C and $R_{VI/II} = 47.1$ and (b) a 0.88 μm thick ZnS epilayer deposited at 342 °C and $R_{VI/II} = 27.7$

emission (Y_0-1 LO) appears at 2.573 eV. Wolf et al. reported these emissions for ZnSe epilayers having total impurity concentrations below 10^{15} cm^{-3}.

Fig. 5b shows the 10 K near band-egde PL emission of a ZnS epilayer deposited at 342 °C and $R_{VI/II} = 27.7$. The dominant feature of the spectrum is the peak at 3.790 eV (I_2) which can be ascribed to a neutral donor bound exciton emission (Kawakami et al.). As for the ZnSe spectrum above, the I_2 line is related to unintentional Cl contamination into the epilayers. Cl atoms originate from residual halides contaminating the alkyl sources, namely the Zn source (Lovergine et al., to be published). A weaker peak (X_{lh}) appears on the high energy side of the I_2 transition, which can be identified with the light-hole (LH) free exciton emission, the heavy-hole (HH) contribution appearing as a faint shoulder on the high energy side of the X_{lh} line. Such labelling is supported by the analysis of the near band-edge absorption spectrum reported by Fernàndez et al. The small energy splitting between LH and HH emissions is due to residual strain in the ZnS layers (Leo et al.). The high optical quality of the ZnS epilayers is further confirmed by the small values of the 10 K absorption line broadenings, equal to 5.2 and 5.6 meV for the LH and HH resonances, respectively (Fernàndez et al.). In the PL spectrum of Fig. 5b two peaks appear at 3.744 eV (I_2-1 LO) and 3.737 eV (I_1), the former being the LO phonon replica of the I_2 line, whereas the latter is ascribed to a neutral acceptor bound exciton line, its LO phonon replica being appearent at 3.695 eV. Finally, a broad emission band can be detected at 3.667 eV ((e, A^0) in Fig. 5b) originat-

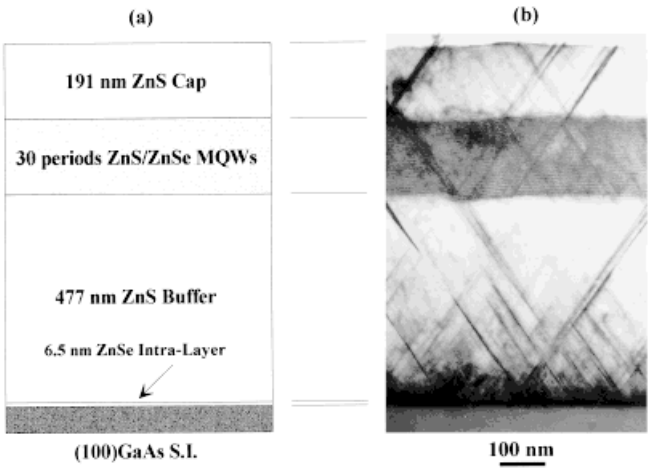

Fig. 6. (a) a scheme of the ZnS/ZnSe MQW-based heterostructure and (b) ⟨011⟩ cross-sectional TEM micrograph of the grown structure showing the appearence of extended defects

ing from a free to bound acceptor transition, followed by its LO phonon replica at 3.624 eV.

ZnS/ZnSe MQWs were thus grown under optimized MOVPE conditions in order to investigate their electronic, optical and structural properties. Fig. 6a reports a scheme of the MQW-based heterostructures. 30 periods ZnS/ZnSe MQWs, having their ZnSe well and ZnS barrier thicknesses equal to 5 ML and 30 ML, respectively, were grown on top of a 477 nm thick ZnS buffer layer and followed by the growth of a 191 nm thick ZnS cap layer. In order to limit the interdiffusion at the quantum well interfaces, both the MQWs structure and the cap layer were grown at a relatively low temperature (315 °C); on the contrary, a higher growth temperature (342 °C) was chosen for the buffer layer, in order to achieve a better crystalline quality of the ZnS epilayer. The above conditions, along with the use of a 10 sec growth interruption time at each ZnS/ZnSe interface during the MQWs growth, have proven to lead to optimized optical properties for the MQW heterostructures (Mazzer et al.). The ZnS buffer was deposited onto the GaAs substrate after the growth of a very thin (6.5 nm) ZnSe intralayer. As the thickness of this intralayer is well below the critical value for plastic relaxation, it does not introduce dislocations at its interface with GaAs; however, it chemically separates the GaAs substrate from ZnS, thus preventing the possible formation of gallium sulphides at the interface between the two materials, which is considered to be detrimental for the crystalline perfection of the ZnS/GaAs heterostructure. Fig. 6b shows a cross-section TEM micrograph of the MQW structure reported in Fig. 6a. TEM analysis shows that planar defects, which lye along the {111} planes and exhibit fringe contrast, propagate through the entire heterostructure. After Chen and Stobbs, some of these defects have been identified as microtwins (MTs), rather than stacking faults (SFs), as MTs and SFs are so closely structurally related that both intrinsic and extrinsic SFs may be regarded as one- and two-layer MTs (Leo et al, 1997). These MTs appear to originate close to the GaAs interface, their density being very high within the first 200−300 nm from the substrate, after which their number decreases to a constant level as they propagate through the whole of the epitaxial structure, up to the MQWs and into the cap layer. Preliminary high resolution TEM observations of the ZnS/ZnSe/GaAs interface region

confirm that these MTs originate at the ZnS/ZnSe interface, the 6.5 nm thick ZnSe intralayer being coherently grown onto the GaAs substrate. Furthermore, both 60°- and 90°-type misfit dislocations appear at the ZnS/ZnSe interface, along with partial dislocations bounding SFs and MTs, demonstrating that all observed defects originate from the plastic relaxation of the ZnS buffer layer, whose thickness is well beyond its critical value for the relaxation of the +4.6% lattice misfit between ZnS and GaAs. As a matter of fact, Leo et al. (1997) have shown that the 477 nm thick ZnS buffer should be almost totally relaxed but for a residual small thermal strain, such that ZnSe/ZnS MQWs structures would grow pseudomorphically on ZnS. Finally, threading dislocations having a density not in excess of 10^6 cm^{-2} are observed into our samples, although they remain confined into the ZnS buffer layer.

Despite the complex defect structure exhibited by the present MQWs, their optical quality has demonstrated to be excellent. Fig. 7 shows the 10 K absorption and PL spectra of a typical 30 periods ZnSe/ZnS MQWs grown under the optimized conditions illustrated above. The absorption spectrum exhibits a clear step-like density of states with superimposed excitonic resonances. The energy positions of these excitonic features were compared with values calculated by means of a Kronig-Penney model as a function of the conduction band discontinuity and taking into account the band shifts induced by a −4.35% residual compressive strain into the ZnSe wells (Lovergine et al, unpublished) and the mass non-parabolicity. An exciton binding energy in the 30−40 meV range was also taken into account (Gil et al.). The inset of Fig. 7 shows the ZnS/ZnSe quantum well band structure resulting from the above calculations: a conduction to valence band offset ratio of 8 : 92 was neccessary to reproduce the absorption features (Cingolani et al.) observed in the experimental spectrum of Fig. 7. The $n = 1$ electron (e1), HH (hh1)

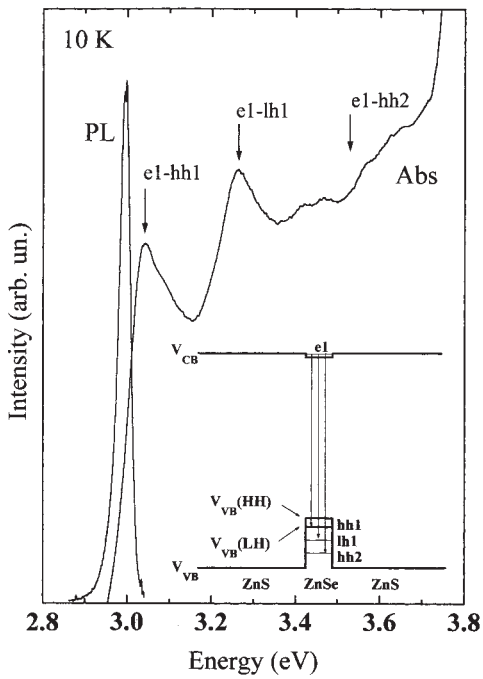

Fig. 7. 10 K absorption and PL spectra of the ZnSe/ZnS MQW structure shown in Fig. 6b. The inset shows the calculated MQW band structure. Electron (e), HH (hh) and LH (lh) related energy levels in the conduction and valence bands are indicated. The numbers 1 and 2 stands for the $n = 1$ or $n = 2$ quantum states in the wells. V_{CB}, V_{VB} (HH) and V_{VB} (LH) represent the conduction and valence band offsets, respectively. The main absorption transitions are also indicated by arrows in the inset and above the absorption spectra

and LH (lh1) and the $n = 2$ HH (hh2) energy levels in the conduction and valence bands, respectively, are also indicated in the Figure inset, along with the expected absorption transitions. The calculated energy positions of these transitions are indicated by the arrows in Fig. 7 and can be compared with the corresponding positions of the excitonic resonances in the experimental absorption spectrum. It turns out that the two peaks at 3.048 eV and 3.26 eV can be identified with the $n = 1$ electron-to-HH and the $n = 1$ electron-to-LH transitions, respectively. However, the additional dipole-forbidden transition involving the $n = 1$ electron and the $n = 2$ HH states forecasted at around 3.55 eV is too weak to be seen in the spectrum. The 10 K cw luminescence spectrum of the MQWs is reported in the same Figure and exhibits a sharp peak at around 3.01 eV with a linewidth of about 28 meV (Mazzer et al.), which corresponds to a Stokes shift (with respect to the fundamental absorption transition) of about 45 meV. Both these values are quite good for an ultrathin quantum well structure and are among the best reported for this material heterostructure (Shen et al).

A study of the MQW PL emission as a function of temperature show that its peak intensity sharply decreases at temperatures above 50 K. This effect is paralleled by an equally sharp reduction of the excitonic features in the high temperature absorption spectra, which appear featureless for temperatures above 170 K. This behaviour has been demonstrated (Cingolani et al.) to be caused by the thermal activation of the electron escaping from the ZnSe wells, such effect being induced by the weak confining potential experienced by the electrons in the present quantum wells. Indeed, our Kronig-Penney calculations have shown that the confinement energy for the electron ground state amounts to only 50 meV, thus explaining the observed thermal quench of the PL and absorption spectra.

Fig. 8 shows the 10 K emission spectra of ZnSe/ZnS MQWs as a function of the excitation power density in the 40−350 kW/cm^2 range. At the lowest excitation power density (curve

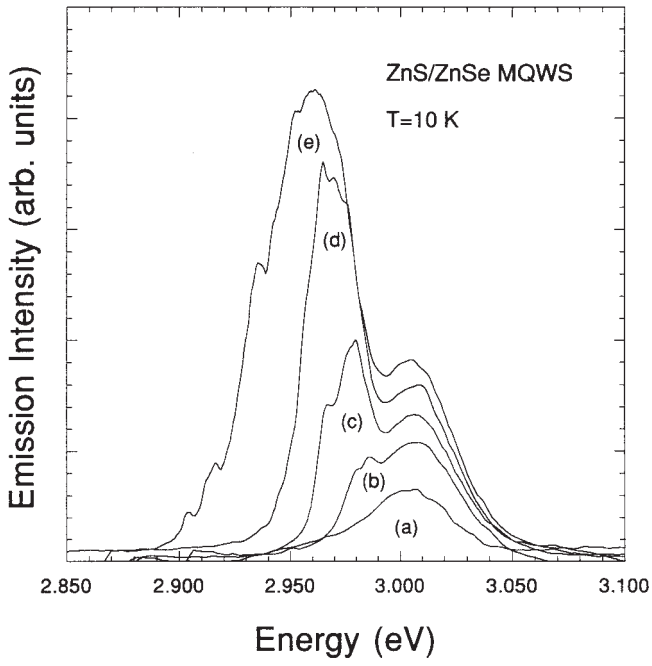

Fig. 8. High excitation PL spectra at 10 K of ZnSe/ZnS MQWs as a function of the excitation power density: (a) 40 kW/cm^2, (b) 100 kW/cm^2, (c) 130 kW/cm^2, (d) 200 kW/cm^2, (e) 350 kW/cm^2

(a)) the luminescence emission is similar to the cw PL spectra with a relatively sharp excitonic recombination at 3.005 eV and a full with at half maximum value of about 40 meV. As the excitation intensity is increased, a condition for population inversion between quantum well states is reached and lasing occurs. This is clearly shown in the spectrum (b) in which the stimulated emission emerges as a sharp peak at 2.959 eV under an excitation power density of about 100 kW/cm^2. By further increasing the excitation power density the stimulated emission intensity increases superlinearly. Also, its peak energy position strongly redshifts as a function of excitation intensity (curves (c)–(e)) due to the effect of band-gap renormalization. Moreover, the linewidth of the stimulated emission broadens as the pump intensity increases as a result of the excitation of many longitudinal modes.

The negligible electron confinement ascribed to the MQWs is reflected in the behaviour of the power density threshold to achieve stimulated emission as a function of temperature, as it increases from the above reported value of 100 kW/cm^2 at 10 K up to around 1000 kW/cm^2 at the maximum temperature of 200 K, above which the sample surface is damaged by the photopumping. Also, the intensity of the stimulated emission rapidly quenches at relatively low temperatures, further confirming the modest electron confinement of the ZnS/ZnSe quantum well system (CINGOLANI et al.).

Conclusions

We reported on the growth by low-pressure MOVPE of ZnS, ZnSe and ZnS/ZnSe MQWs heterostructures using high purity ^{t}BuSH, ^{t}Bu$_2$Se and the adduct Me$_2$Zn:Et$_3$N, as S, Se and Zn precursors, respectively. The effect of the different growth parameters on the growth rates and structural properties of the epilayers has been evidenced. In particular, by growing under high VI/II molar flow ratios, the occurrence of residual pre-reactions between ^{t}BuSH and Me$_2$Zn:Et$_3$N can be suppressed, thus achieving unprecedentedly reported high structural and optical quality ZnS epilayers. High VI/II ratios were also used for ZnSe layers, showing that these conditions are not detrimental for their structural quality. Indeed, the crystallinity of both ZnS and ZnSe could be greatly improved under reduced growth rates (below 1 μm/hr) or by keeping the growth temperature in the 340–370 °C range, indicating that the kinetics of the incorporation of Zn, S and Se species at the growing surface is the underlying mechanism that limit the materials lattice perfection. Dominant (excitonic) band-edge emissions were also reported for these epilayers, showing that the total amount of unintentional impurities is always very low. Cl originating from the Zn alkyl source has been recognized as the main background impurity into both ZnS and ZnSe.

The excellent quality achieved by the materials grown under the above MOVPE conditions allowed us to match the stringent requirements needed to achieve high quality ZnS/ZnSe MQWs. Their structural properties under optimized growth conditions were shown to be limited mostly by the formation of extended defects (such as microtwins), a result of the high lattice mismatch involved into the ZnS/ZnSe heterostructure. Despite the large amount of microtwins found, the optical quality of the MQWs turned out to be high, which made possible the full characterization of their electronic and lasing properties. In particular, lasing emission up to 50 K were reported from the present MQWs heterostructures in the 3.0 eV (i.e., 413 nm) energy range.

However, it is evident that a proper exploitation of the ZnS/ZnSe MQWs as a lasing system need a substantial improvement of their electron confinement, which can be

achieved by the use of MgZnS alloys instead of ZnS as a barrier material. MgZnS/ZnSe heterostructures might have also the adventage of increasing the total band gap discontinuity, while preserving the binary nature of the ZnSe quantum well.

More work is on progress in our laboratory, focussing on both the MOVPE growth and the characterization of Mg-containing materials in order to further explore the potentials of II−VI based systems having competing performances with respect to the III-nitrides for the realization of LDs operating into the 400 nm wavelength region of the visible spectrum.

Acknowledgments

The authors would like to ackowledge L. Lazzarini and G. Salviati of MASPEC-CNR for performing the TEM observations and for useful discussions. Also, the technical assistance of D. Cannoletta, A. Melcarne and A. Pinna is acknowledged.

References

Gil, B., Cloitre, T., Di Blasio, M., Bigenwald, P., Aigouy, L., Briot, N., Briot, O., Bouchara, D., Aulombard, R. L., Calas, J.: Phys. Rev. **B50** (1994) 18231

Chen, C. Y., Stobbs, W. M.: Ultramicroscopy **58** (1995) 289

Cingolani, R., Prete, P., Lomascolo, M., Coli', G., Calcagnile, L., Lovergine, N., Salviati, G., Lazzarini, L.: Appl. Phys. Lett. **70** (1997) 2943

Fernàndez, M., Prete, P., Lovergine, N., Mancini, A. M., Cingolani, R., Vasanelli, L., Perrone, M. R.: Phys. Rev. **B55** (1997) 7660

Gebhardt, W., et al.: J. Cryst. Growth (1995)

Giannini, C., Peluso, T., Gerardi, C., Tapfer, L., Lovergine, N., Vasanelli, L.: J. Appl. Phys. **77** (1995) 2429

Hahn, B., Kastner, M., Preis, H., Schindler, M., Gebhardt, W.: 7th European Workshop on MOVPE and Related Growth Techniques, Berlin (D), June 8−11, 1997

Haase, M. A., Qiu, J., Depuydt, J. M., Cheng, H.: Appl. Phys. Lett. **59** (1991) 1272

Kahn, O., O'Brien, P., Hamilton, P., Walsh, J., Jones, A. C.: Chemtronics **4** (1989) 244

Kawakami, Y., Taguchi, T., Hiraki, A.: J. Cryst. Growth **89** (1988) 331

Kuhn, W., Naumov, A., Stanzl, H., Bauer, S., Wolf, K., Wagner, H.P., Gebhardt, W., Pohl, U. W., Krost, A., Richter, W., Dümichen, U., Thiele, K. H.: J. Cryst. Growth **123** (1992) 605

Irvine, S.J.C., Stafford, A., Maung, N.: Appl. Phys. Lett. (1996)

Leo, G., Lovergine, N., Prete, P., Longo, M., Cingolani, R., Mancini, A. M., Romanato, F., Drigo, A. V.: J. Cryst. Growth **159** (1996) 144

Leo, G., Lazzarini, L., Lovergine, N., Romanato, F., Drigo, A. V.: J. Cryst. Growth **173** (1997) 277

Lovergine, N., Longo, M., Gerardi, C., Manno, D., Mancini, A. M., Vasanelli, L.: J. Cryst. Growth **156** (1995) 45

Mazzer, M., Calcagnile, L., Leo, G., Salviati, G., Zanotti-Fregonara, C., Lovergine, N., Prete, P., Imbriani, G., Cingolani, R., Mancini, A. M., Romanato, F., Drigo, A. V.: Mater. Sci. Engineer. **B43** (1997) 97

Nakamura, S., Senoh, M., Magahama, S.-I., Iwasa, N., Yamada, T., Matsushita, T., Kiyoku, H., Sugimoto, Y.: Jap. J. Appl. Phys. **35** (1996) L74

Nishimura, K., Sakai, K., Nagao, Y., Ezaki, T.: J. Cryst. Growth **117** (1992) 119

Shahzad, K., Petruzzello, J., Olego, D. J., Cammack, D. A., GAINES, J. M.: Appl. Phys. Lett. **57** (1990) 2452

Wolf, K., Jilka, S., Sahin, H., Stanzl, H., Reisinger, T., Naumov, A., Gebhardt, W.: J. Cryst. Growth **152** (1995) 34

Taguchi, T., Kawakami, Y., Yamada, Y.: Physica B **191** (1993) 23

Wright, P. J., Cockayne, Parbrook, P. J., Jones, A. C., O'Brien, P., Walsh, J. R.: J. Cryst. Growth **104** (1990) 601

Shen, A., Wang, H., Wang, Z.: Appl. Phys. Lett. **60** (1992) 2640